IFT18

A MATTER OF SCIENCE+FOOD

Event: July 15-18
Food Expo: July 16-18
Chicago, IL
McCormick Place
IFTEVENT.ORG

WHY IFT18 MATTERS TO YOU

You need insights, you need to make strategic connections, and you need access. At IFT18, you will get all this and more. Each year, IFT brings the best and brightest from around globe to inspire and challenge the status quo.

A Matter of Science

100+ Scientific Sessions | 11 Pre-event Short Courses

Gain insights, learn skills, get solutions to real-world challenges that impact your work, and meet the people who are driving innovation across the science of food.

A Matter of Connection and Professional Development

20,000 Attendees from 90+ Countries | 40+Recruiters Anxious to Meet You

Attend professional development sessions, networking events, and IFT's Career Center Live to build new relationships with limitless opportunities to learn, connect, and expand your professional ecosystem.

A Matter of Inspiration and Discovery

1000+ Companies

Learn what's next and get business done with the largest and most diverse concentration of global food partners.

A Matter of Innovation and Insight

Provocative IFT*NEXT Sessions and Market Insights**

Be challenged to think big and be bold. Immerse yourself in future forward thinking and insights to gain a better understanding of what the future of food will look like and how you can have an impact.

* IFT*NEXT* is made possible through the generous support of Ingredion, IFT's Platinum Innovation Sponsor.

REGISTER TODAY AND SAVE!

Register today and take advantage of early registration and hotel discounts.
Become a member and save up to 40% on registration.

Learn more at iftevent.org

Structural Modification of Fish Gelatin by the Addition of Gellan, κ-Carrageenan, and Salts Mimics the Critical Physicochemical Properties of Pork Gelatin

Li Cheng Sow, Karmaine Kong, and Hongshun Yang

Abstract: Pork gelatin is not suitable for halal and kosher application; however, fish gelatin (FG) can be modified for use as a pork gelatin (PG) mimetic. Herein, low-acyl gellan (GE), κ-carrageenan (KC), and salts ($CaCl_2$ or KCl) were combined with a 180 Bloom tilapia FG. A formulation comprising 5.925% (w/v) FG + 0.025% (w/v) GE + 3mM $CaCl_2$ best matched the physicochemical properties of PG. The modification increased the FG gel strength from 115 ± 2 to 149 ± 2 g (matching the 148 ± 2 of PG), while the T_m increased from 27.9 ± 1.0 to 32.4 ± 0.8 °C (matching the 33.1 ± 0.3 °C of PG). Nanoaggregates (diameter between 150 and 300 nm) could be an important structural factor affecting the physicochemical properties, as both PG and GE-modified FG showed a similar frequency distribution in this size group (57.4 ± 1.6% (PG) compared with 56.3 ± 2.2% (modified FG)). To further explore the differences between KC and GE in modifying of FG's structure, the FG-KC and FG-GE gels were compared. The zeta potential and Fourier transform infrared (FTIR) spectroscopy results for the FG-KC gel supported an associative interaction with complex formation, as indicated from the large aggregates and amorphous phase under atomic force microscopy (AFM). Contrastingly, a segregative FG-GE interaction took place in presence of $CaCl_2$. These structures and interaction differences between FG-GE and FG-KC influenced the macro-properties of FG, possibly explaining the differences in the modification of the melting temperature of FG. A diagram representing the interaction-structure-physicochemical properties was proposed to explain the differences between the FG-GE and FG-KC gels.

Keywords: atomic force microscopy (AFM), carrageenan, gelatin, gellan, nanostructure

Practical Application: Certain people cannot consume any pork product or derivatives for religious reasons, thus it is essential to find a pork gelatin (PG) substitute for food product development. The commonly used polysaccharides, gellan and carrageenan, together with salt, can be added to fish gelatin (FG) to match the textural properties of PG, representing a promising substitute for PG. The difference in the mechanism of gellan and carrageenan to improve properties of FG has been revealed from nanostructure level. The use of food grade ingredients and simple mixing process are favorable in the food industry.

Introduction

Gelatin is extracted from bones and skins, and is used as a multifunctional ingredient in food (Gomez-Guillen et al., 2009). Most commercial gelatin (>98.5%) available in the market originates from mammalian sources (Gomez-Guillen et al., 2009), which limits the universal use of gelatin to produce halal and kosher certified food (Karim & Bhat, 2008). Given the projected growth in the Muslim population to 30% of world's populace by 2025 (Shafie & Othman, 2006), pork gelatin (PG) alternatives would be valuable to unleash the potential of the expanding halal food market (He & Yang, 2018).

One of the potential substitutes that can fulfill the religious sentiments of consumers is fish gelatin (FG). FG, especially that extracted from warm water fishes such as tilapia, possess similar properties to mammalian gelatin, except that the gel strength, melting temperature (T_m), and gelling temperature (T_g) could be lower (Zhou, Mulvaney, & Regenstein, 2006; Gilsenan & Ross-Murphy, 2000). These attributes are economically significant because the commercial value of gelatin is largely based on its gel strength, while the T_m and T_g determine its food applications (Karim et al., 2008). It was predicted that if fish gelatin could be used as mammalian gelatin alternative, seafood processing waste could be reduced by fish gelatin extraction, thereby improving seafood sustainability and food security (Feng, Bansal, & Yang, 2016; Feng, Ng, Mikš-Krajnik, & Yang, 2017a).

FG modification can minimize the physicochemical differences between FG and mammalian gelatin. A method employing mixing of salts or polysaccharides with gelatin is a common, practical, and consumer friendly approach in the food industry because of its ease of application, reduced health risk, and lower cost. The type of polysaccharide, salt, and their mixing ratio in FG will determine the effective property modifications of gelatin. Gum arabic, dextran, carboxy-methylcellulose, inulin, and guar gum

JFDS-2017-1613 Submitted 9/28/2017, Accepted 2/22/2018. *Authors are with Food Science and Technology Programme, c/o Dept. of Chemistry, National Univ. of Singapore, Singapore. Authors are also with National Univ. of Singapore (Suzhou) Research Inst., 377 Lin Quan Street, Suzhou Industrial Park, Suzhou, Jiangsu, P.R. China. Direct inquires to author Yang (E-mail: chmynghs@nus.edu.sg).*

doi: 10.1111/1750-3841.14123

Journal of Food Science A Publication of the Institute of Food Technologists

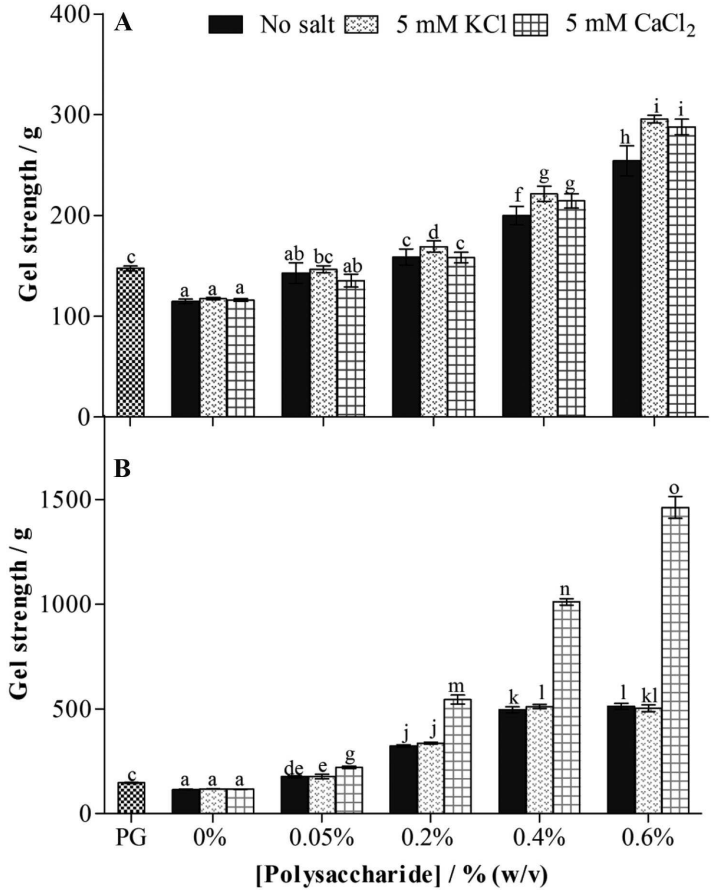

Figure 1–Effect of the concentration of (A) κ-carrageenan (KC) and (B) low-acyl gellan (GE) and salt type on the gel strength of fish gelatin (FG) compared with pork gelatin (PG). *Groups with different letters indicate statistical difference ($P < 0.05$). *Polysaccharide was added to replace FG from a 6% gelatin gel (w/v); the FG-polysaccharide gel had a total biopolymer concentration of 6% (w/v).

Table 1–Gel strength and TPA of FG/GE/$CaCl_2$ and FG/KC/KCl gels.

Type	Salt	Gel strength (g)	Hardness (N)	Springiness (%)	Cohesiveness (%)	Chewiness (N)
PG	–	148 ± 2^{d}	15.9 ± 0.6^{c}	88.6 ± 0.8^{a}	95.4 ± 1.6^{e}	13.4 ± 0.7^{c}
FG	–	115 ± 2^{a}	12.8 ± 0.7^{a}	90.7 ± 1.5^{bc}	93.1 ± 1.1^{d}	10.8 ± 0.7^{a}
FG + 0.025% GE	0 mM $CaCl_2$	143 ± 3^{c}	16.4 ± 0.6^{cd}	89.6 ± 1.3^{ab}	90.7 ± 2.7^{c}	13.4 ± 0.9^{c}
	3 mM $CaCl_2$	149 ± 2^{d}	15.9 ± 0.6^{c}	88.7 ± 0.6^{a}	87.7 ± 1.6^{a}	12.4 ± 0.7^{b}
	5 mM $CaCl_2$	159 ± 3^{e}	17.5 ± 0.5^{e}	89.6 ± 0.5^{ab}	88.1 ± 1.4^{ab}	13.8 ± 0.5^{c}
FG + 0.040% GE	0 mM $CaCl_2$	146 ± 2^{cd}	17.1 ± 1.1^{de}	90.5 ± 1.9^{bc}	89.2 ± 1.2^{abc}	13.8 ± 1.1^{c}
FG + 0.18% KC	0 mM KCl	136 ± 3^{b}	14.9 ± 0.6^{b}	88.7 ± 1.0^{a}	90.4 ± 2.1^{c}	12.0 ± 0.8^{b}
	5 mM KCl	146 ± 5^{cd}	16.6 ± 0.9^{cd}	88.6 ± 0.6^{a}	90.0 ± 2.5^{bc}	13.3 ± 1.1^{c}
	10 mM KCl	148 ± 4^{d}	17.6 ± 0.7^{e}	88.6 ± 0.8^{a}	90.1 ± 1.4^{bc}	14.0 ± 0.8^{c}
FG + 0.20% KC	0 mM KCl	146 ± 4^{cd}	17.1 ± 0.6^{de}	90.9 ± 1.4^{c}	89.7 ± 1.2^{bc}	13.9 ± 0.5^{c}

*Within each column, groups with different lower case letters indicate statistical difference ($P < 0.05$) among the groups.
*FG: Fish gelatin; GE: Low acyl-gellan; KC: κ-carrageenan.

(Harrington & Morris, 2009) were ineffective in increasing the T_m, T_g, or gel strength of gelatin. However, κ-carrageenan, gellan (Pranoto, Lee, & Park, 2007), and alginate (Panouillé & Larreta-Garde, 2009) have been reported to improve the physicochemical properties of gelatin.

However, the previous reports did not focus on the mechanism underlying the modification of the physicochemical properties. It was reported that mixing of biopolymers could result in associative or segregative interactions and affect the developed structure (de Kruif, Weinbreck, & de Vries, 2004). The main objective of the study was to reveal the underlying mechanism that resulted in the difference FG modifications based on structure (nanostructure and secondary structure) and interaction. In this study, we used tilapia gelatin, a commercially available warm-water FG that has a higher gel strength, T_m, and T_g compared with FG derived from cold-water fish (Karim & Bhat, 2009). Recently, our group also applied tilapia FG in seafood to improve its texture, nutrient retention, and shelf life (Feng et al., 2016, 2017a, Feng, Fu, & Yang, 2017b; Sow et al., 2017), tilapia FG also been applied in low fat-stirred yogurt and successfully mimic properties of bovine gelatin (Pang, Deeth, Yang, Prakash, & Bansal, 2017). In the present study, FG mixed with κ-carrageenan (KC) and low-acyl gellan (GE) for the use as a pork gelatin mimetic were prepared, the physicochemical properties and structure modification were compared. The mechanisms of the modification of FG's physicochemical properties were further explored at the structural and interaction levels.

Table 2–T_m and T_g of pork gelatin (PG), fish gelatin (FG) and the modified FG (FGG, FGG+, FGK, FGK+).

Sample	T_m (°C)	T_g (°C)
PG	33.1 ± 0.3[c]	24.2 ± 0.5[c]
FG	27.9 ± 1.0[a]	18.3 ± 0.1[a]
FGG	29.2 ± 0.1[b]	18.6 ± 0.4[a]
FGG+	32.4 ± 0.8[c]	19.7 ± 2.5[ab]
FGK	29.2 ± 0.6[b]	19.9 ± 0.3[ab]
FGK+	30.0 ± 0.6[b]	20.7 ± 0.1[b]
#1.5% KC + 5 mM KCl	43.2 ± 0.01[d]	30.5 ± 0.5[d]
#0.2% GE + 3 mM $CaCl_2$	>70	N.D.

*Within each column, groups with different lower case letters indicate statistical difference ($P < 0.05$) among the groups.
*FGG (FG + 0.040% GE), FGG+ (FG + 0.025% GE + 3 mM $CaCl_2$), FGK (FG + 0.20 % KC) and FGK+ (FG + 0.18% KC + 5 mM KCl).
#The condition of KC and GE was the minimally required gelling condition that was placing the samples in 4 ± 2 °C refrigerator overnight. No melting of GE gel was detected from 10 to 70 °C, thus no gelation of GE (10 to 70 °C) was detected (N.D.).

Materials and Methods

Materials

Commercial 180 Bloom tilapia fish gelatin (FG) and 240 Bloom pork gelatin (PG) were obtained from Jiangxi Cosen Biology Co., Ltd (Yingtan, Jiangxi, China) and Qingdao Huachang Food Ingredients Co. Ltd (Qingdao, Shandong, China), respectively. Low-acyl gellan (GE) and κ-carrageenan SeaKem® CM 611 (KC) were a gift from FMC Health and Nutrition (Philadelphia, PA, U.S.A.). From intrinsic viscosity determination and Mark-Houwink equation (Bohidar, 1998; Dreveton, Monot, Lecourtier, Ballerini, & Choplin, 1996; Vreeman, Snoeren, & Payens, 1980), the viscosity averaged molecular weight of FG, PG, GE and KC were estimated to be 47765, 29617, 87037, and 78488 g/mol, respectively. The counterions contents (Ca, Na, K) of FG, PG, GE, and KC were showed in Table S1. Potassium chloride (KCl) and dihydrate salt of calcium chloride ($CaCl_2 \cdot 2H_2O$) were purchased from Merck KGaA (Damstadt, Germany). Fluorescein isothiocyanate (FITC) and rhodamine B, dimethyl sulfoxide (DMSO) were purchased from Sigma-Aldrich (St. Louis, Mo., U.S.A.).

Gel preparation

The total polymer concentration of gelatin and modified FG gels were fixed at 6% (w/v). Dried gelatin granules were hydrated in deionized water for 2 hr and subsequently heated and shaken for 10 min in a 65 °C water bath (Sow & Yang, 2015). For FG-polysaccharide gels, FG and polysaccharides (KC and GE) were separately hydrated by dividing the amount of deionized water 1:1 (v/v). The polysaccharides were stirred and heated to 90 °C for GE and 65 °C for KC until completely dissolved. The polysaccharide solutions were then added to the FG solution and stirred for another 10 min. KCl and $CaCl_2$ (<10 mM) were added to the mixture of FG-polysaccharides when necessary. The solutions were filled into flat-bottomed cylindrical jars (2.5 cm diameter, 3.1 cm height) and allowed to form gel by storing at 8 ± 2 °C for 17 ± 1 hr before measurements.

Gel strength and texture profile analysis (TPA)

Gel strength measurements and TPA of the gels were carried out using a TA.XT2-i Texture Analyser (Stable Micro System, Goldaming, Surrey, UK) (Sow & Yang, 2015). Gels were equilibrated to 10 °C and removed from the container before the measurement. For gel strength, a P/0.5R cylindrical plunger was used with test speed of 0.5 mm/s and gel penetration distance of 4 mm. Two-cycle compression TPA at 40% compression was carried out using a 47 mm diameter flat plate. TPA parameters of hardness, cohesiveness, springiness, and chewiness were obtained from the compression curve, according to the definition in Yang et al. (2007).

Melting temperature (T_m) and gelling temperature (T_g)

T_m and T_g of the gel samples were studied using rheological methods modified from Boran, Mulvaney, and Regenstein (2010). Gel samples were cut into 2.5 cm diameter circular discs and placed on a TwinDrive™ Rheometer (Anton Paar, Oreg., U.S.A.) with parallel plate geometry (2.5 cm diameter); the thickness of the gel was 1 mm. The T_m and T_g of the samples were determined with temperature sweep from 10 to 40 °C (for T_m), followed by 40 to 10 °C (for T_g) at a scan rate of 1 °C/min, a frequency of 1 Hz, and stress of 3 to 5 Pa; the elastic modulus (G') and loss modulus (G") were recorded. T_m and T_g were calculated as temperature where the crossover of G' and G" occurred. Before the temperature sweeps, the frequency and stress sweep tests were conducted from 0.1 to 10 Hz and 0.1 to 1000 Pa at 10 °C to confirm that the applied stress and frequency of the temperature sweep were within the linear viscoelastic range.

Atomic force microscopy (AFM)

AFM imaging was carried out using a TT-AFM (AFM workshop, Signal Hill, CA, U.S.A.) equipped with an AppNano ACLA-10 probe (Applied NanoStructures, Mountain View, CA, U.S.A.). Samples were diluted to 0.2% (w/v) with deionized water, dried on mica sheet, and imaged; the resonance frequency of the probe was 145 KHz; the force constant was 25 to 95 N/m; and the scan speed used was 0.4 Hz (Sow et al., 2017). The images were processed and analyzed using Gwyddion software (https://gwyddion.net). The dimensions of the spherical aggregates were obtained by line profile extraction.

Zeta (ζ) potential

ζ-potential measurements were carried out according to the methods outlined by Wu and McClements (2015), with slight modifications. Hot solutions (6 %, w/v) were diluted with hot deionized water to 0.1 % (w/v), followed by shaking for 2 hr at 25 °C prior to analysis. Phase analysis light scattering (PALS) mode was selected for the ζ-potential measurements at 25 °C, using the NanoBrook Omni Particle Size and Zeta Potential analyzer (Brookhaven Instruments, NY, U.S.A.), The Smoluschowski equation was applied to calculate the ζ-potential.

Fourier transform infrared (FTIR) spectroscopy

Gel samples were lyophilized, milled, and combined with KBr (3 mg sample per 97 mg KBr) for FTIR spectroscopy (Sow & Yang, 2015). Spectral data were collected using a Spectrum One FTIR spectrometer (PerkinElmer, Waltham, MA, U.S.A.), from 4000 to 450 cm^{-1}, at 4 cm^{-1} resolution and a scan number of 64. Background spectrum was collected before every sample spectra, the spectra were baseline corrected and smoothened using the Spectrum software (version 5.0.1, PerkinElmer). Fourier self-deconvolution was also carried out using the Spectrum software with the settings of line narrowing factor, 1.5 Gamma and smoothing length width of 50 %. Gaussian curve fitting of the Amide I band was performed between 1600 and 1700 cm^{-1} using OriginPro 2015 (OriginLab, Northampton, MA, U.S.A.). The final fit of all samples had a corrected $R^2 > 0.98$.

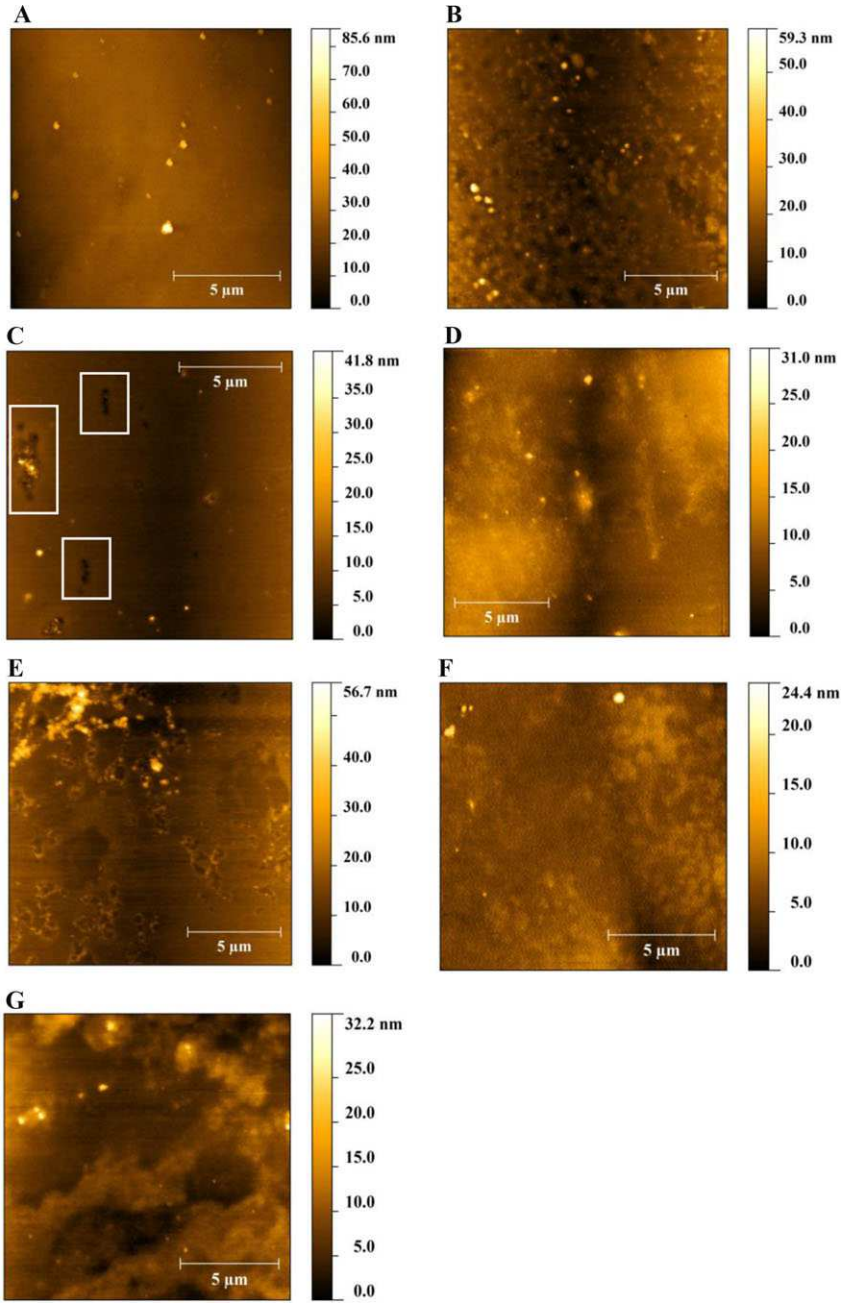

Figure 2–Representative nanostructures of gelatin spherical aggregates from (A) pork gelatin (PG) and (B) fish gelatin (FG); (C) irregular pores from fish gelatin + 0.04% gellan (FGG); (D) amorphous phase with aggregates from FGG; (E) chain like aggregates and pores from fish gelatin + 0.025% gellan + 3 mM $CaCl_2$ (FGG+); (F) amorphous phase with aggregates from fish gelatin + 0.2% κ-carrageenan (FGK); (G) distinct amorphous phase of fish gelatin + 0.18% κ-carrageenan + 5 mM KCl (FGK+).

Confocal laser scanning microscope

FG, GE, and KC were labelled by fluorescent marker, rhodamine B (FG) and FITC (GE & KC) according to the method modified from Razzak, Kim, and Chung (2016). Rhodamine B has a excitation/emission wavelengths of 540/625 nm (red) while that of FITC is 490/525 nm (green). FG, GE and KC solution (0.5 %, w/v) were individually prepared, to facilitate binding of the dye, the pH of FG was adjusted to 10.5 while GE and KC to 8.5, 25 μL of 2 % (w/v) dyes in DMSO were added into 100 mL of biopolymer solutions, the solutions were stirred for 90 min at room temperature. At the end of 90 min, the pH of the mixtures was adjusted back to original pH, Rhodamine B-labelled FG and FITC labelled-GE or KC were mixed together. The sample was pipetted on a 1-mm-thick glass cover slide, covered and stored at 10 °C overnight. Microstructure of the droplet was captured by an Olympus FV1000 confocal scanning unit (Tokyo, Japan) equipped argon ion and HeNe laser, the images were taken at a magnification of 60x with water immersion. The images were processed using Olympus Fluoview software.

Statistical analysis

Three independent experiments were performed with at least triplicate samples within each run. For AFM, dozens of parallel images were used to obtain statistically reliable data on the feature dimensions. The results were reported as mean values ± standard deviations. Differences between groups were determined using one-way ANOVA ($P < 0.05$) and Duncan's multiple range test,

Table 3–Summary of the nanostructure of different gelatin samples.

	PG	FG	FGG	FGG+	FGK	FGK+
Spherical aggregate	+	+	+	+	+	+
Diameter (nm)	197 ± 97[a]	204 ± 93[a]	333 ± 259[c]	256 ± 103[b]	320 ± 150[c]	390 ± 194[d]
Height (nm)	8.4 ± 9.7[a]	8.1 ± 8.3[a]	6.9 ± 7.2[a]	8.5 ± 7.0[a]	14.6 ± 38.7[b]	13.8 ± 19.6[b]
Irregular aggregate	+	+	+	+	+	+
Annular pore	+	+	+	+	+	+
Irregular pore	−	−	+	+	+	+
Amorphous structure	−	−	+	+	+	+
Ring-like structure	+	+	+	+	+	+

*FGG (FG + 0.040% GE), FGG+ (FG + 0.025% GE + 3 mM $CaCl_2$), FGK (FG + 0.20 % KC) and FGK+ (FG + 0.18% KC + 5 mM KCl).
*Within each row, groups with different lower case letters indicate statistical difference ($P < 0.05$).
* "+" indicates the presence of a structure. "−" indicates the absence of a structure.

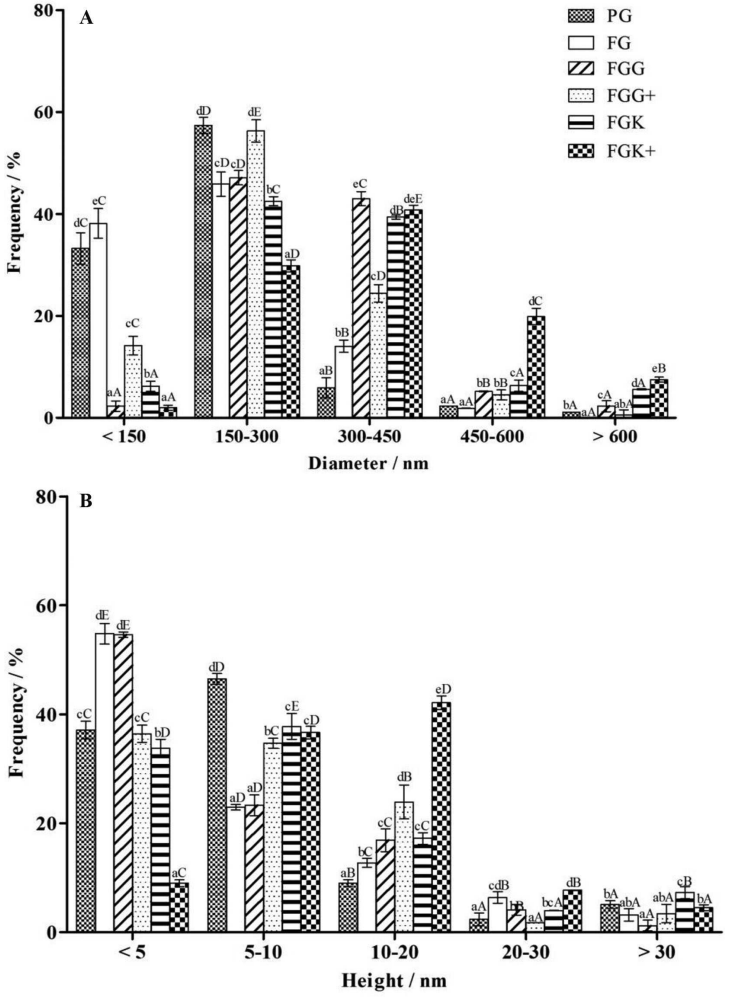

Figure 3–Frequency histogram for (A) the diameter of the spherical aggregates; (B) the height of the spherical aggregates. *Within each size range, groups with different lowercase letters were statistically different ($P < 0.05$). Within each sample, groups with different capital letters showed statistical difference ($P < 0.05$). *FGG (FG + 0.040% GE), FGG+ (FG + 0.025% GE + 3 mM $CaCl_2$), FGK (FG + 0.20 % KC) and FGK+ (FG + 0.18% KC + 5 mM KCl). PG: Pork gelatin; FG: Fish gelatin; GE: Low acyl-gellan; KC: κ-carrageenan.

performed using the SPSS Statistics 20 software (IBM, Chicago, IL, U.S.A.).

Results and Discussion

Gel strength and TPA

The texture parameters of PG were used as the target reference for the modification of FG. Textural properties modification of FG is shown in Figure 1 and Table S1. FG displayed a statistically lower gel strength, hardness, cohesiveness, and chewiness compared with PG ($P < 0.05$). Two polysaccharides, KC and GE (0 to 0.6 %, w/v) and two types of salts (KCl, $CaCl_2$) were mixed with FG, the biopolymer concentration of the mixed gel was fixed at 6 % (w/v). As the polysaccharide concentration increased, gel strength, hardness, and chewiness of FG increased (Figure 1 and Table S1). In contrast, gel cohesiveness and springiness were reduced by the addition of KC and GE (Table S1). This could be due to the double helices of the polysaccharide gels (GE and KC) are more rigid and stiff than the triple helices of gelatin (Mao, Tang, & Swanson, 2001). Therefore, there was a need to limit the concentration of

Table 4–ζ-potential and pH of different gelatins samples.

	ζ-Potential (mV)	pH
PG	12.3 ± 1.1[a]	5.62 ± 0.01[e]
FG	9.1 ± 0.6[b]	6.22 ± 0.10[bc]
FGG	6.0 ± 0.3[c]	6.16 ± 0.02[cd]
FGG+	7.3 ± 0.3[d]	6.12 ± 0.01[cd]
FGK	2.6 ± 0.4[e]	6.33 ± 0.01[b]
FGK+	1.4 ± 0.3[f]	6.23 ± 0.01[bc]
0.2% (w/v) GE	–37.3 ± 3.2[g]	6.07 ± 0.02[d]
0.2% (w/v) KC	–50.7 ± 2.0[h]	6.87 ± 0.01[a]

*FGG (FG + 0.040% GE), FGG+ (FG + 0.025% GE + 3 mM $CaCl_2$), FGK (FG + 0.20 % KC) and FGK+ (FG + 0.18% KC + 5 mM KCl).
*The samples were diluted from 6% to 0.1% (w/v).
*Within each row, groups with different lower case letters indicate statistical difference ($P < 0.05$).
*The isoelectric point of PG and FG was pH 7.92 and pH 7.79, respectively (Figure S1).

polysaccharides in mixed gel. At the same polysaccharide concentration, GE delivered more pronounced changes in gel strength than KC (Figure 1). In particular, FG-GE gels surpassed the gel strength of PG gels at 0.05% GE, while FG-KC gels matched the gel strength of PG gels at 0.20% KC. This could be attributed to the structure and molecular weight differences of GE and KC. Unlike the alternating (1→3) and (1→4) linked KC, GE displayed longer stretches of (1→4) di-equatorial linkages, which are related to flat, rigid structures (Morris, Nishinari, & Rinaudo, 2012). The molecular weight of GE also greater than KC.

KCl and $CaCl_2$ at 5 mM were added to all samples (Figure 1 and Table S1). There was no significant difference ($P > 0.05$) for all texture parameters of FG with 5 mM $CaCl_2$ or KCl in comparison to FG alone. In the mixed FG-GE and FG-KC gels, the textural changes dependent on the salt type. For the FG-GE gels, $CaCl_2$ was more effective than KCl in increasing the gel strength at all observed GE concentrations. This effect was caused by the direct crosslinking of two GE chain by Ca^{2+} compared with that of the long range, indirect coordination of K^+ (Morris et al., 2012). For the FG-KC gels, KCl was slightly more effective than $CaCl_2$ in terms of gel strength and texture modification at 0.05% and 0.20% KC. This observation agreed with the report of Piculell (2006) that the ion selectivity of KC reflected the helix cavity sizes of the KC chain, which accommodated larger cations (K^+) better than smaller cations (Ca^{2+}).

To develop a PG substitute, an optimization experiment was carried out based on the screening results. The GE concentration was reduced below 0.05% to bring the gel strength and hardness closer to those of PG, while KC concentrations between 0.05% and 0.20% were further explored to optimize the texture properties of the FG-KC gel. In terms of the effect of salt, $CaCl_2$ (≤5 mM) was chosen as the additive in the FG-GE gels, based on the superior effect in increasing gel strength and textural properties, while KCl salt addition was explored at ≥5 mM in the FG-KC gels. Selected results from the optimization experiment are summarized in Table 1.

Table 1 shows that FG with 0.04% GE mimicked the gel strength of PG ($P > 0.05$) and had a similar TPA. With the addition of $CaCl_2$ at 3 mM, the GE concentration in the FG-GE gel could be reduced to 0.025% to achieve the objective of mimicking the texture of PG. By contrast, KC at 0.2% in the FG-KC gel was required to attain a similar gel strength and TPA to PG. The addition of KCl was effective at 5 mM for the FG-KC gels, allowing the concentration of KC to be reduced slightly 0.2% to 0.18%, resulting in a close match of the texture to PG.

Thus, based on the gel strength and TPA results, four FG-polysaccharide formulations (with and without salt) were selected based on statistically similar gel strengths ($P > 0.05$) and similar TPA to PG: FG + 0.040% GE (FGG), FG + 0.025% GE + 3 mM $CaCl_2$ (FGG+), FG + 0.20% KC (FGK), and FG + 0.18% KC + 5 mM KCl (FGK+).

Melting temperature (T_m) and gelling temperature (T_g)

The T_m and T_g of PG, FG, and the four selected formulations (FGG, FGG+, FGK, and FGK+) based on gel strength and TPA were subject to rheological measurement, the results are summarized in Table 2. Gelatin gels are known for their unique "melt-in-mouth" sensation, which arises from a T_m slightly lower than the human body temperature (Karim et al., 2008). The T_m and T_g of PG were at least 5 °C higher than the corresponding temperatures of FG, which was similar to the observation from Zhou et al. (2006). All four FG-polysaccharides formulations showed an increase in the T_m relative to the FG gel, with FGG+ showing the largest increase in T_m of about 4.5 °C. Among the selected formulations, only FGG+ attained a T_m of 32.4 ± 0.8 °C which was statistically similar ($P > 0.05$) to PG. The T_m is related to the amount of energy required to break the cross-linked junction zones (Derkach, Ilyin, Maklakova, Kulichikhin, & Malkin, 2015), thus there could be a stronger junction zone formation or increases in number of junction zones. There was no significant improvement in the T_g of the FGG, FGG+, and FGK relative to FG. FGK+ was the only sample that displayed a statistically significant increase in the T_g relative to FG, although the T_g (20.7 ± 0.1 °C) was still lower than that of the PG gel.

In short, FGG+ was the only formulation that matched the T_m of PG. As the T_m determines gel storage conditions and is crucial in flavor release through the "melt-in-mouth" perception, together with its similarity of gel strength and TPA properties, the FGG+ formulation with 0.025% gellan + 5.975% FG + 3 mM $CaCl_2$ showed potential as a PG mimetic.

Nanostructure by AFM

The nanostructures of the unmodified gelatin (FG, PG) as well as the modified FGs (FGK, FGK+, FGG, FGG+) were compared under AFM (Figure 2). Heterogeneous nanostructures were identified and summarized in Table 3. AFM imaging was carried out at low concentrations of 0.2%; therefore, spherical and irregular aggregates (the common features for low concentration of gelatin at <1%) were observed in all samples (Yang & Wang, 2009).

The aggregates (Figure 2) resulted from multimeric association of biopolymers, where aggregates were stabilized by electrostatic interactions, hydrogen bonding, and Van der Waals forces (Lin et al., 2002). The aggregation state of gelatin molecules is related to their macroscale structure (Yang, 2014). Pores (Figure 2C and E) were formed via evaporation of water that penetrated into the gelatin and the conglomeration of gelatin outside the sphere of water (Yang & Wang, 2009). Amorphous structures (Figure 2D, F, G) were observed in the FG-polysaccharides, though they were more common in FGG, FGK, and FGK+, but not in FGG+. The amorphous structures were identified as complex-coacervates formed between FG and the polysaccharides. Previously, Mohanty and Bohidar (2005) described Type B gelatin coacervates observed from AFM imaging as portions of dense matter with no definite geometric features. Sow et al. (2017) also reported an amorphous structure of fish gelatin and gellan that associated as one phase. In dilute conditions, coacervation was attributed to associative interactions between oppositely charged polymers (de

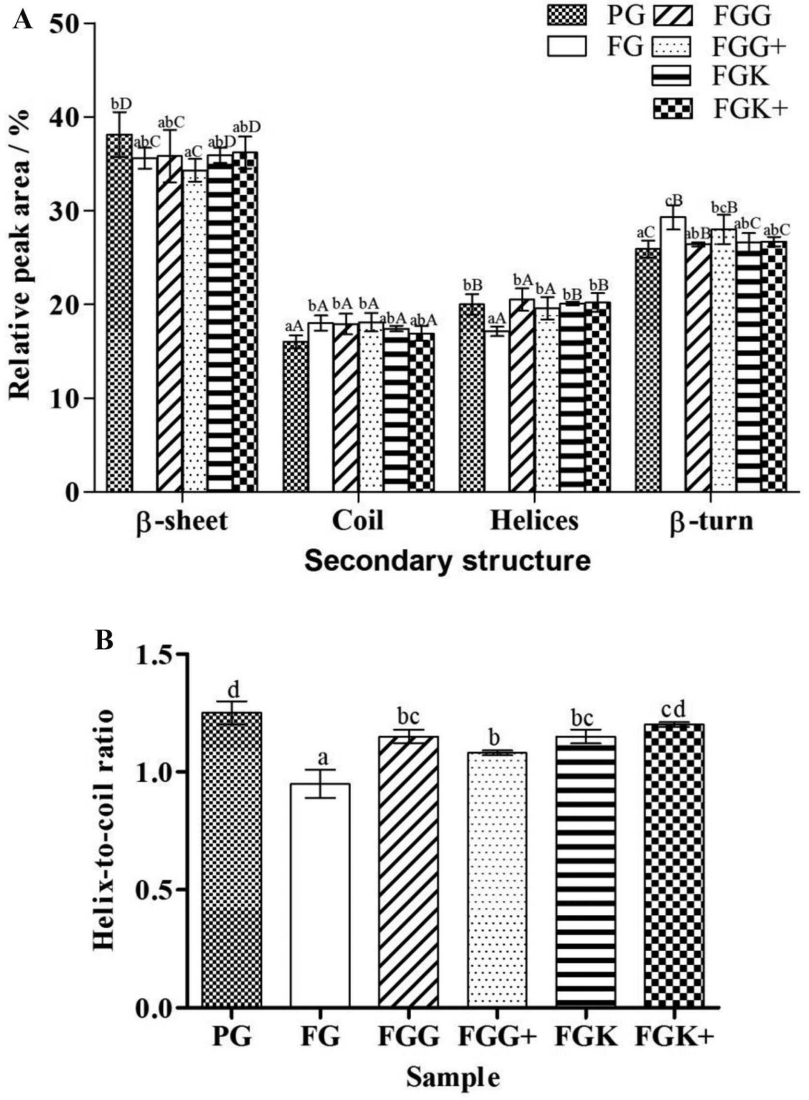

Figure 4–Amide I deconvolution featuring (A) the relative peak area of secondary structures; (B) the helix-to-coil ratio. *Within same type of secondary structure, groups with different lowercase letters were statistically different ($P < 0.05$). Within each sample, groups with different capital letters were statistically different ($P < 0.05$).

Kruif et al., 2004). The formation of coacervates was reported between gelatin-GE mixtures (Hans Tromp, van de Velde, van Riel, & Paques, 2001) and gelatin-KC mixtures (Fang, Li, Inoue, Lundin, & Appelqvist, 2006). Particularly, the more distinct coacervates of FGK and FGK+ might suggested the increased prevalence of associative interactions between FG and KC.

For further quantification, commonly observed spherical aggregates were measured for their diameter and height distributions (Table 3 and Figure 3). From Table 3, the average diameters of the PG and FG aggregates were statistically similar at 197 ± 97 and 204 ± 93 nm, respectively. This was consistent with the findings of Saxena, Sachin, Bohidar, and Verma (2005) who found that the diameter of PG aggregates was between 200 and 300 nm. Similarly, Sow and Yang (2015) reported the diameter of tilapia FG aggregates to be 201 ± 115 nm. The average aggregate diameter increased significantly ($P < 0.05$) in the FG-GE and FG-KC gels. In increasing order (Table 3), the aggregate diameters were FGG+ (256 ± 103 nm) < FGG (333 ± 259 nm) ≈ FGK (320 ± 150 nm) < FGK+ (390 ± 194 nm). Aggregate heights were PG ≈ FG ≈ FGG ≈ FGG+ < FGK ≈ FGK+. The diameter of the FG-gellan mixture, with or without $CaCl_2$, was similar to the report of Sow et al. (2017). Interestingly, the dimension of the aggregates seemed to correlate with the occurrence of the amorphous structure, among which the samples with more a distinct amorphous structure (FGK, FGK+) comprised larger spherical aggregates, further supporting the view that there could be associative complex formation, resulting in the formation of large aggregates and an amorphous phase.

The size distribution frequencies (Figure 3) could be meaningful to further explore the differences in the structure. Although the average diameter and height of the spherical aggregates from PG and FG were not significantly different ($P > 0.05$), the size distribution frequencies were different. In the diameter group (150 to 300 nm), FG had a lower frequency (45.9 ± 2.4%) compared with PG (57.4 ± 1.6%), while for the height distribution in the 0–5 nm region, FG displayed greater aggregate height distributions than PG. Interestingly, only FGG+ matched the frequency (56.3 ± 2.2%) of PG in the 150 to 300 nm diameter group and 0–5 nm height group (36.4 ± 1.6% in FGG+ compared with 37.1 ± 1.6% in PG). This suggested that aggregates of 150 to 300 nm in diameter and 0 to 5 nm in height could be important for the structural modification of FG that is critical to the final

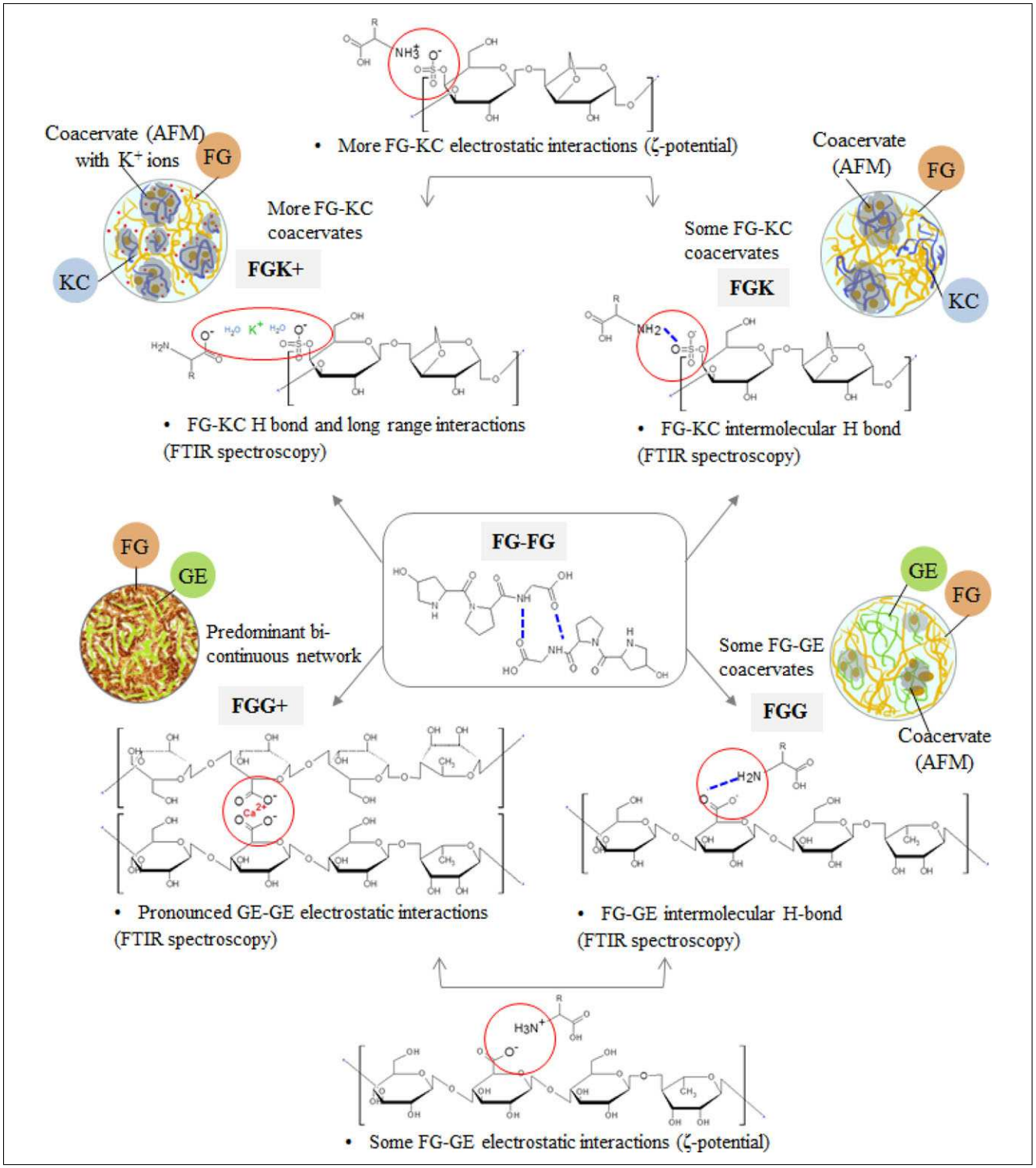

Figure 5–Schematic diagram depicting the modification of fish gelatin (FG). *FGG (FG + 0.040% GE), FGG+ (FG + 0.025% GE + 3 mM $CaCl_2$), FGK (FG + 0.20 % KC) and FGK+ (FG + 0.18% KC + 5 mM KCl). PG: Pork gelatin; FG: Fish gelatin; GE: Low acyl-gellan; KC: κ-carrageenan.

modification of the physicochemical properties. Almost all samples showed highest frequencies distribution in the group of diameters between 150 and 300 nm, except for FGK+, which had the highest frequency in the diameter group of 300 to 500 nm. While for the FG-KC gel, other mechanisms, likely involving large associative complex formation, might be responsible for the modifications to the FG physicochemical properties.

Zeta (ζ) potential

Measurement of the ζ-potential provides information regarding the surface charges of biopolymers. The changes in the ζ-potential in the FG-GE and FG-KC gels also served as an indication of electrostatic interaction between gelatin and the polysaccharides (Razzak et al., 2016). From Table 4, PG displayed a statistically higher positive ζ-potential (12.3 $\pm$ 1.1 mV) than FG (9.1 $\pm$ 0.6 mV),

Table 5–Peak position and assignment from FTIR spectra.

Region	Peak wavenumber (cm^{-1}) PG	FG	FGG	FGG+	FGK	FGK+	Description
Amide A	3336.6 ± 2.8^{b}	3335.7 ± 2.3^{b}	3330.7 ± 1.9^{a}	3338.3 ± 0.5^{b}	3331.2 ± 0.7^{a}	3331.1 ± 0.9^{a}	NH stretch coupled with H-bond
Amide B	3084.0 ± 0.5^{ab}	3084.8 ± 0.1^{b}	3084.2 ± 0.4^{ab}	3083.7 ± 0.2^{a}	3084.8 ± 0.8^{b}	3084.4 ± 0.4^{ab}	NH bend
Amide I	1661.1 ± 1.9^{a}	1660.9 ± 1.8^{a}	1662.1 ± 0.6^{a}	1662.0 ± 1.6^{a}	1662.5 ± 0.9^{a}	1661.6 ± 0.4^{a}	C = O stretch/ NH bend
Amide II 1	1552.5 ± 0.4^{a}	1553.2 ± 0.4^{a}	1553.1 ± 0.5^{a}	1552.9 ± 0.4^{a}	1552.5 ± 1.6^{a}	1551.7 ± 1.2^{a}	CN stretch and NH bend
2	1453.1 ± 0.5^{a}	1453.0 ± 0.3^{a}	1452.9 ± 0.2^{a}	1452.8 ± 0.2^{a}	1453.1 ± 0.4^{a}	1453.1 ± 0.1^{a}	CH_2 bend
3	1404.1 ± 0.2^{b}	1403.8 ± 0.2^{ab}	1403.7 ± 0.2^{a}	1404.2 ± 0.3^{b}	1403.7 ± 0.4^{a}	1403.9 ± 0.2^{ab}	COO^{-} symmetrical stretch
4	1338.0 ± 0.4^{a}	1338.1 ± 0.3^{a}	1337.5 ± 0.4^{a}	1338.0 ± 0.5^{a}	1337.7 ± 0.5^{a}	1337.9 ± 0.3^{a}	CH_2 wag (proline and glycine)
Amide III	1240.4 ± 0.3^{b}	1240.2 ± 0.1^{ab}	1240.4 ± 0.3^{b}	1239.8 ± 0.3^{a}	1240.5 ± 0.2^{b}	1240.3 ± 0.3^{b}	NH deformation/ CN stretch
Fingerprint1	1082.2 ± 0.1^{b}	1082.0 ± 0.1^{b}	1082.1 ± 0.1^{b}	1082.2 ± 0.1^{b}	1081.2 ± 0.2^{a}	1081.1 ± 0.1^{a}	C–O skeletal stretch
2	1032.6 ± 0.1^{a}	1032.7 ± 0.2^{a}	1032.6 ± 0.0^{a}	1032.8 ± 0.1^{a}	1033.7 ± 0.3^{b}	1033.7 ± 0.1^{b}	C–O skeletal stretch
3	973.8 ± 0.1^{b}	973.6 ± 0.2^{b}	973.9 ± 0.1^{b}	973.8 ± 0.3^{b}	973.1 ± 0.1^{a}	973.2 ± 0.3^{a}	C–O skeletal stretch
4	938.0 ± 0.3^{b}	937.9 ± 0.2^{b}	938.0 ± 0.3^{b}	938.5 ± 0.4^{b}	934.6 ± 1.1^{a}	934.7 ± 0.5^{a}	C–O skeletal stretch

*FGG (FG + 0.040% GE), FGG+ (FG + 0.025% GE + 3 mM $CaCl_2$), FGK (FG + 0.20 % KC), FGK+ (FG + 0.18% KC + 5 mM KCl).
*Within each row, groups with different lower case letters indicate statistical difference ($P < 0.05$).

possibly due to the lower pH of PG than FG. Both PG and FG carried net positive charges as the pH were above isoelectric point (pH 7.79 for FG and 7.92 for PG). GE and KC were strongly anionic, as shown by their highly negative ζ-potentials of -37.3 ± 3.2 and –50.7 ± 2.0 mV, respectively. Thus, the charge density of KC was confirmed to be higher than GE, because of the presence of a large number of anionic sulfated groups compared with the carboxylic acid groups of GE (de Jong & others, 2007).

Electrostatic interactions are highly probable for oppositely charged polyelectrolytes (that is, weakly positive FG and strongly negative GE or KC). Upon the addition of GE and KC to FG, a significant ($P < 0.05$) decrease in the ζ-potential was observed. A lower ζ-potential was observed for FGK and FGK+ samples (2.6 ± 0.4 and 1.4 ± 0.3 mV, respectively) relative to FGG and FGG+ samples (6.0 ± 0.3 and 7.3 ± 0.3 mV, respectively), this was expected as the concentration of KC added (0.18% to 0.2%, w/v) were about 10 times more than that of GE (0.025% to 0.04%, w/v). The reduced ζ-potential after FG modification confirmed the presence of associative electrostatic interactions between FG and GE or KC, where the anionic polysaccharides neutralized the positive surface charges on FG (Cao et al., 2015). Wu et al. (2015) also reported decreases in the ζ-potential during gelatin (weakly cationic) and OSA-starch (anionic) complexation via electrostatic interactions.

Interestingly, the effect of salt was opposite in FG-GE and FG-KC. Upon $CaCl_2$ addition, the ζ-potential of FGG+ significantly increased compared with that of FGG. In contrast, the addition of KCl decreased the ζ-potential of FGK+ compared with that of FGK. The effect could be explained as $CaCl_2$ interacted with GE and formed strong, direct crosslinking of the GE-GE chains. The crosslinking interaction interfered with the FG-GE associative complexation, and fewer negatively charged GE chains were associated with positively charged FG, hence increased the ζ-potential. By contrast, the addition of KCl might promote a stronger associative interaction between FG-KC and further reduce the ζ-potential. The results of ζ-potential measurement supported the observation of AFM where there could be more distinct associative complex coacervation in FGG, FGK, and FGK+ than in FGG+.

FTIR spectroscopy

The peaks from the FTIR spectra (Figure S2) were identified and presented in Table 5. Overall, the FTIR spectra pattern showed characteristics of gelatin spectra of PG and tilapia FG reported by Nur Hanani, Roos, and Kerry (2012) and Sow and Yang (2015), respectively. The addition of KC modified the fingerprint region of the spectra, which was attributed to strong absorption peaks by the 3,6-anhydro-D-galactose groups and glycosidic linkages of KC at 930 and 1010 to 1080 cm^{-1}, respectively (Pereira, Sousa, Coelho, Amado, & Ribeiro-Claro, 2003; Yang, Yang, & Yang, 2018).

The Amide A band was related to —NH stretching vibration coupled to intramolecular hydrogen bonding (Pranoto et al., 2007), and significant shifting of amide A was observed upon FG modification. FGG, FGK, and FGK+ displayed a shift to a lower wavenumber relative to FG alone. The shift to a lower wavenumber indicated the occurrence of associative intermolecular hydrogen bonding (Myshakina, Ahmed, & Asher, 2008) between —OH and/or $—COO^{-}$ (for GE, FG), —OH (for KC), and the —NH group of FG, the hydrogen bond could be formed between FG and polysaccharides or within FG-FG or polysaccharides-polysaccharides alone. The presence of hydrogen bonding between fish gelatin and gellan was also observed by Sow et al. (2017).

By contrast, the amide A band of FGG+ was shifted to a higher wavenumber, probably because the presence of Ca^{2+} ions interfered with the intermolecular hydrogen bonding between FG and GE. Instead, stronger bonds, such as electrostatic interactions, could form and shorten the bond length of the -NH functional group, thus increasing the wavenumber (Pal, Banthia, & Majumdar, 2007). In support, Verma and Pandit (2012) reported shifts to higher wavenumbers in GE hydrogel beads because of strong electrostatic attractions between GE and Ca^{2+} cations. The increase in the GE-GE electrostatic interaction by Ca^{2+} led to segregative interactions between FG and GE.

No significant shifting of Amide I shift was observed for all modified FGs. To further elucidate sample differences, deconvolution of the Amide I band was carried out to estimate the proportion of secondary structures in gelatin and the extent of protein conformational change (Sow & Yang, 2015). The component peaks were assigned to the secondary structures of β-sheet, coil, helix, and β-turn (Kong & Yu, 2007; Sow & Yang, 2015). The average wavenumber of the component peaks was 1621.4 ± 0.6 and 1636.3 ± 0.9 cm^{-1} for β-sheets, 1646.3 ± 1.5 cm^{-1} for random coils, 1660.3 ± 0.9 cm^{-1} for helices, 1671.4 ± 2.0 and 1684.0 ± 0.7 cm^{-1} for β-turns. The component peak percentages are shown in Figure 4.

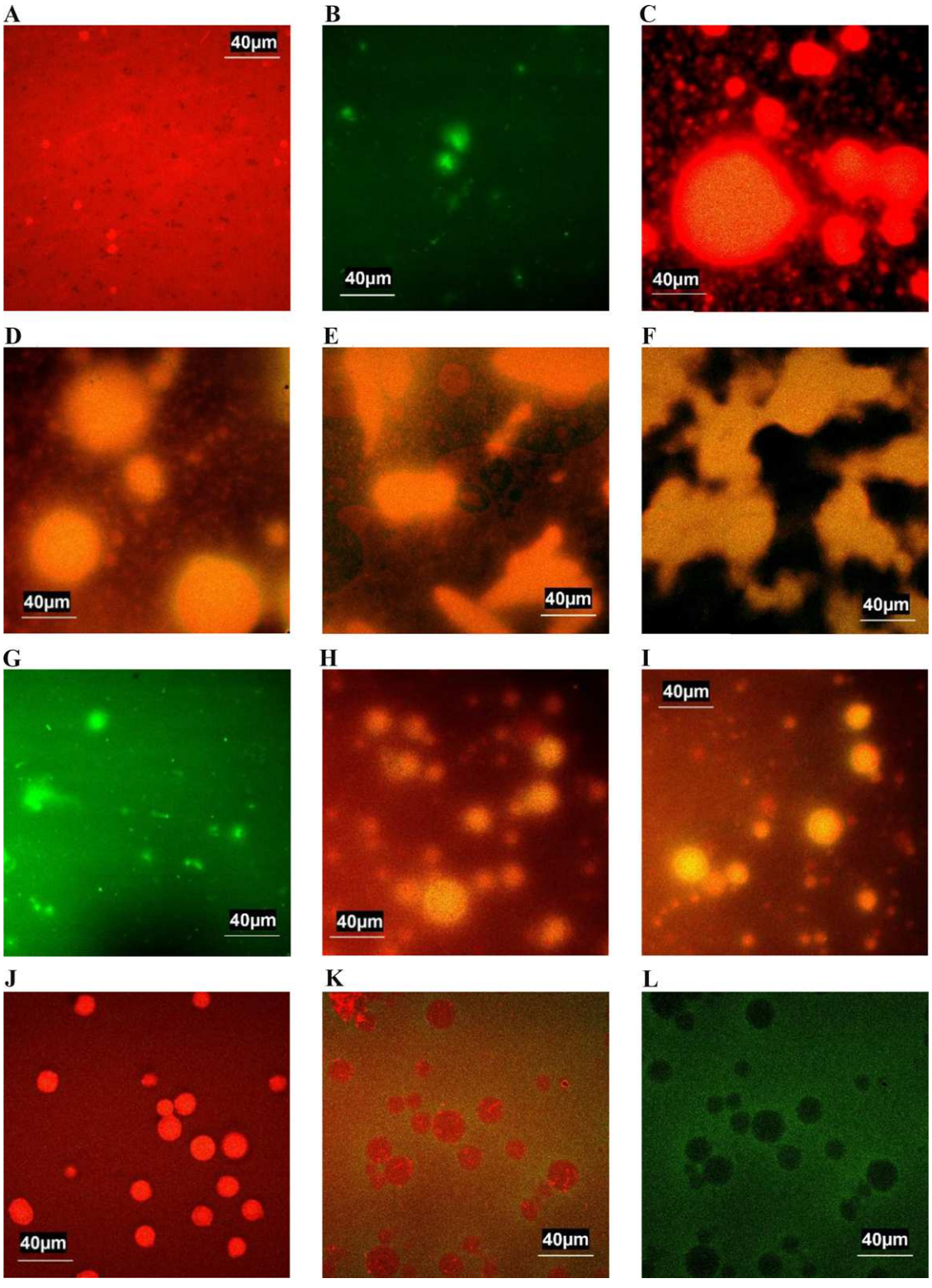

Figure 6–CLSM images of (A) FG, (B) KC, (C & D) FGK, (E & F) FGK+, (G) GE, (H & I) FGG, (J, K & L) FGG+, image (L) is obtained from the green FITC channel of image (K) to highlight the segregation behavior of FG in FGG+ mixture.

From Figure 4(A), PG, FGK, and FGK+ each showed a relative abundance of secondary structures in the following the ascending order: disordered coil < helix < β-turn < β-sheet. For FG, FGG, and FGG+, the secondary structures followed the ascending order of: disordered coil ≈ helix < β-turn < β-sheet. The abundance of β-turns and β-sheets were consistent with a previous report (Muyonga, Cole, & Duodu, 2004). Compared with FG, all modified samples had a higher helix percentage; FGG and FGG+

displayed a statistically similar disordered coil percentage, while FGK and FGK+ showed a lower disordered coil percentage. The area percentage ratio of helix to random coil components was calculated (Figure 4B). The helix-to-coil ratio was used to estimate the triple helix content in gelatin (Weng, Zheng, & Su, 2014), where a low helix-to-coil ratio indicated low triple helix content.

The comparison of unmodified PG and FG revealed that PG possessed a higher helix-to-coil ratio (1.25 ± 0.05) than FG (0.95 ± 0.06). This suggested that the lower gel strength, hardness, chewiness, T_m and T_g of FG relative to PG was related to the low helix-to-coil ratio of FG, possibly because of the role of the triple helix as a junction zone for the formation of a continuous, three-dimensional network (Gilsenan & Ross-Murphy, 2000). Furthermore, the helix-to-coil ratios of the four modified FG (FGG, FGG+, FGK, and FGK+) were statistically higher than that of FG. Polysaccharides promoted triple helix formation in the modified FG gels by providing stabilizing intermolecular hydrogen bonds to the triple helix (Karim et al., 2009). Segregative behavior of FG-polysaccharides might also improve triple helix formation, as FG-FG was allowed to position closer to each other due to the excluded volume effect and repulsion of polysaccharides chains (Nieto Nieto et al., 2016), therefore increased in opportunity of hydrogen bond assisted triple helix formation and stabilisation.

Interaction–structure–physicochemical properties relationship

The results from the different aspects of the FG-polysaccharides gels including physicochemical properties (gel strength, TPA, T_m, and T_g), interaction (ζ-potential & FTIR), and structure (FTIR and AFM), were combined to produce a proposed schematic model (Figure 5) of the relationship of these three aspects of the gels. The model served to illustrate the difference in the mechanism of GE and KC in the modification of FG and the success of FGG+ as a PG substitute. The structures were attributed to gelatin-polysaccharide, gelatin-gelatin, and polysaccharide-polysaccharide interactions, the modification in structures in turn contributed to the physicochemical properties.

For example, hydrogen bonding (indicated by a blue dash in Figure 5) was prominent in the FG-FG, FGK, and FGG systems, which was supported by the FTIR results (mainly amide A, helix-to-coil ratio). When K^+ shielded the negatively charged patches of KC or FG, additional long-range interactions could be established on top of the hydrogen bonds in FGK. Moreover, two types of electrostatic interactions were found between FG (NH_3^+) and polysaccharides ($-OSO_3^-$, $-COO^-$) or between the Ca^{2+}-crosslinked GE-GE chains, which was supported by the ζ-potential analysis and FTIR results. The FG-KC systems were highly associated with the effect of hydrogen bonding, electrostatic interaction, and the long-range associative interaction by the shielding effect of K^+. While for the FG-GE system, FGG has a greater degree of associative interactions than FGG+. This is because when Ca^{2+} was involved, the strong GE–GE electrostatic interaction reduced some of the GE that previously associated with FG.

As a result of differences in the interactions, the structure of FGG+ also differed from those of FGK, FGK+, and FGG. Complex coacervation observed under AFM suggested the formation of a mixed gel in FGK, FGK+, and FGG. The coacervates size of FGK and FGK+ were larger than that of FGG, as the amount of KC added was also greater than the amount of GE. The weight ratio of FG was more than 97% in all FG-polysaccharides gels; therefore, the remaining FG that was not bound to polysaccharides could also contribute to the structure and gel network formation. With the segregative interaction in FGG+, a bi-continuous network could form, first by the Ca^{2+-} crosslinked GE-GE network, followed by formation of the FG-FG network when cooling.

It is important to emphasize the impact of these nanostructures on the macroscopic gel physicochemical properties. On a nanoscale, the packing efficiency of the aggregates was related to the physicochemical properties of the gels (Yu, Yan, Han, & Huang, 2013). The textural properties of all FG-polysaccharides gel (FGG, FGG+, FGK, and FGK+) were similar to each other and to PG, while a more pronounced difference was noted for the T_m of the gels. While gel rigidity (gel strength, hardness) can be attributed to complex coacervates and the mixed gel formation alone, the bi-continuous phase formation in FGG+ resulted in the largest improvement in the T_m. The involvement of the Ca^{2+}-crosslinked GE-GE network contributed to higher T_m. In addition, the similar aggregate size distributions of FGG+ and PG (at 150 to 300 nm diameter, 0 to 5 nm height) suggested similar packing of the nano-aggregates in the macroscopic 3D-gel network, thus making FGG+ the best match in terms of melting temperature (T_m) to PG compared with the other formulations (FGG, FGK, and FGK+), with equivalent gel strength.

CLSM

In order to confirm the structure modification as proposed in schematic model (Figure 5), the microstructure images of CLSM were shown in Figure 6. FG was covalently labeled with Rhodamine B (red) while GE and KC were labeled with FITC dye (green). The control images were shown in Figure 6(A), (B), (G) for FG, KC and GE (0.5%, w/v), respectively. Large complex coacervates were observed in FGK (Figure 6C and D) and FGK+ (Figure 6E and F), in which the complex coacervates of FGK+ were more prominent, non-uniform and interconnected than FGK. For FGG, small spherical complex coacervates were observed (Figure 6H and I). FGG+ samples showed small spherical aggregates that were mainly contributed by FG, of which the segregative behavior was highlighted in Figure 6J. The image from GE (green FITC) channel showed void of "spherical aggregates" that further supported the spherical aggregates were mainly FG (red, Figure 6I), this could serve as evidence of the segregative behavior in FGG+.

Conclusions

The combination of polysaccharides and salts with FG produced a PG mimetic based on critical properties, including the gel strength and melting temperature of gelatin. Of the various formulations with equivalent gel strength, the FGG+ formulation of 180 Bloom FG + 0.025% (w/v) gellan + 3 mM $CaCl_2$ (for a 6% (w/v) total polymer concentration) successfully matched the gel strength and T_m of 240 Bloom PG. The successful matching of physicochemical properties was supported by structure and interaction analysis, where Ca^{2+} changed the associative FG-GE system to a segregative FG-FG/ GE-GE system, which eventually led to a bi-continuous network. In addition, FGG+ was the only formulation that displayed a similar aggregate size distribution to PG in the AFM nanostructure studies, which could be extrapolated into similar packing of the 3D gel network, resulting in similar physicochemical properties. With the successful preparation of a FG-based pork gelatin mimetic, this study showed promise in formulating a PG replacer to meet the religious needs of people.

Acknowledgments

We thank the financial support from projects 31471605 and 31371851 supported by NSFC, Singapore Ministry of Education Academic Research Fund Tier 1 (R-143-000-583-112) and a project from Fujian Putian Sea-100 Food Co., Ltd (R-143-000-633-597).

Author Contributions

L.C. Sow collected the experimental data, interpreted the results and drafted the manuscript. K. Kong collected the data of physicochemical properties and AFM structural characterization. H. Yang designed the experiment and revised the manuscript.

References

Bohidar, H. B. (1998). Hydrodyamic properties of gelatin in dilute solutions. *International Journal of Biological Macromolecules*, *23*, 1–6.

Boran, G., Mulvaney, S. J., & Regenstein, J. M. (2010). Rheological properties of gelatin from silver carp skin compared to commercially available gelatins from different sources. *Journal of Food Science*, *75*, E565–E571.

de Jong, S., & van de Velde, F. (2007). Charge density of polysaccharide controls microstructure and large deformation properties of mixed gels. *Food Hydrocolloids*, *21*, 1172–1187.

de Kruif, C. G., Weinbreck, F., & de Vries, R. (2004). Complex coacervation of proteins and anionic polysaccharides. *Current Opinion in Colloid & Interface Science*, *9*, 340–349.

Derkach, S. R., Ilyin, S. O., Maklakova, A. A., Kulichikhin, V. G., & Malkin, A. Y. (2015). The rheology of gelatin hydrogels modified by κ-carrageenan. *LWT - Food Science and Technology*, *63*, 612–619.

Dreveton, E., Monot, F., Lecourtier, J., Ballerini, D., & Choplin, L. (1996). Influence of fermentation hydrodynamics on gellan gum physico-chemical characteristics. *Journal of Fermentation and Bioengineering*, *82*, 272–276.

Fang, Y., Li, L., Inoue, C., Lundin, L., & Appelqvist, I. (2006). Associative and segregative phase separations of gelatin/κ-carrageenan aqueous mixtures. *Langmuir*, *22*, 9532–9537.

Feng, X., Bansal, N., & Yang, H. (2016). Fish gelatin combined with chitosan coating inhibits myofibril degradation of golden promfret (*Trachinotus blochii*) fillet during cold storage. *Food Chemistry*, *200*, 283–292.

Feng, X., Fu, C., & Yang, H. (2017b). Gelatin addition improves the nutrient retention, texture and mass transfer of fish balls without altering their nanostructure during boiling. *LWT - Food Science and Technology*, *77*, 142–151.

Feng, X., Ng, V. K., Mikš-Krajnik, M., & Yang, H. (2017a). Effects of fish gelatin and tea polyphenol coating on the spoilage and degradation of myofibril in fish fillet during cold storage. *Food and Bioprocess Technology*, *10*, 89–102.

Gilsenan, P. M., & Ross-Murphy, S. B. (2000). Rheological characterisation of gelatins from mammalian and marine sources. *Food Hydrocolloids*, *14*, 191–195.

Gomez-Guillen, M. C., Perez-Mateos, M., Gomez-Estaca, J., Lopez-Caballero, E., Gimenez, B., & Montero, P. (2009). Fish gelatin: A renewable material for developing active biodegradable films. *Trends in Food Science and Technology*, *20*, 3–16.

Hans Tromp, R., van de Velde, F., van Riel, J., & Paques, M. (2001). Confocal scanning light microscopy (CSLM) on mixtures of gelatine and polysaccharides. *Food Research International*, *34*, 931–938.

Harrington, J. C., & Morris, E. R. (2009). Conformational ordering and gelation of gelatin in mixtures with soluble polysaccharides. *Food Hydrocolloids*, *23*, 327–336.

He, Z., & Yang, H. (2018). Colourimetric detection of swine-specific DNA for halal authentication using gold nanoparticles. *Food Control*, *88*, 9–14.

Karim, A. A., & Bhat, R. (2008). Gelatin alternatives for the food industry: Recent developments, challenges and prospects. *Trends in Food Science and Technology*, *19*, 644–656.

Karim, A. A., & Bhat, R. (2009). Fish gelatin: Properties, challenges, and prospects as an alternative to mammalian gelatins. *Food Hydrocolloids*, *23*, 563–576.

Kong, J., & Yu, S. (2007). Fourier transform infrared spectroscopic analysis of protein secondary structures. *Acta Biochimica et Biophysica Sinica*, *39*, 549–559.

Lin, W., Yan, L., Mu, C., Li, W., Zhang, M., & Zhu, Q. (2002). Effect of pH on gelatin self-association investigated by laser light scattering and atomic force microscopy. *Polymer International*, *51*, 233–238.

Mao, R., Tang, J., & Swanson, B. G. (2001). Water holding capacity and microstructure of gellan gels. *Carbohydrate Polymers*, *46*, 365–371.

Mohanty, B., & Bohidar, H. B. (2005). AFM study of morphology of ethanol induced gelatin coacervation. *International Journal of Polymeric Materials*, *54*, 675–689.

Morris, E. R., Nishinari, K., & Rinaudo, M. (2012). Gelation of gellan – A review. *Food Hydrocolloids*, *28*, 373–411.

Muyonga, J. H., Cole, C. G. B., & Duodu, K. G. (2004). Fourier transform infrared (FTIR) spectroscopic study of acid soluble collagen and gelatin from skins and bones of young and adult Nile perch (*Lates niloticus*). *Food Chemistry*, *86*, 325–332.

Myshakina, N. S., Ahmed, Z., & Asher, S. A. (2008). Dependence of amide vibrations on hydrogen bonding. *Journal of Physical Chemistry B*, *112*, 11873–11877.

Nur Hanani, Z. A., Roos, Y. H., & Kerry, J. P. (2012). Use of beef, pork and fish gelatin sources in the manufacture of films and assessment of their composition and mechanical properties. *Food Hydrocolloids*, *29*, 144–151.

Pal, K., Banthia, A. K., & Majumdar, D. K. (2007). Preparation and characterization of polyvinyl alcohol-gelatin hydrogel membranes for biomedical applications. *AAPS PharmSciTech*, *8*, E142–E146.

Pang, Z., Deeth, H., Yang, H., Prakash, S., & Bansal, N. (2017). Evaluation of tilapia skin gelatin as a mammalian gelatin replacer in acid milk gels and low-fat stirred yogurt. *Journal of Dairy Science*, *100*, 3436–3447.

Panouillé, M., & Larreta-Garde, V. (2009). Gelation behaviour of gelatin and alginate mixtures. *Food Hydrocolloids*, *23*, 1074–1080.

Pereira, L., Sousa, A., Coelho, H., Amado, A. M., & Ribeiro-Claro, P. J. A. (2003). Use of FTIR, FT-Raman and 13C-NMR spectroscopy for identification of some seaweed phycocolloids. *Biomolecular Engineering*, *20*, 223–228.

Piculell, L. (2006). Gelling carrageenans. In A. M. Stephen, G. O. Phillips, & P. A. Williams (Eds.), *Food polysaccharides and their applications* (pp. 239–228). Boca Raton, Fla.: CRC Press.

Pranoto, Y., Lee, C. M., & Park, H. J. (2007). Characterizations of fish gelatin films added with gellan and κ-carrageenan. *LWT - Food Science and Technology*, *40*, 766–774.

Razzak, M. A., Kim, M., & Chung, D. (2016). Elucidation of aqueous interactions between fish gelatin and sodium alginate. *Carbohydrate Polymers*, *148*, 181–188.

Saxena, A., Sachin, K., Bohidar, H. B., & Verma, A. K. (2005). Effect of molecular weight heterogeneity on drug encapsulation efficiency of gelatin nano-particles. *Colloids and Surfaces B: Biointerfaces* , *45*, 42–48.

Shafie, S., & Othman, M. N. 2006. Halal Certification: An international marketing issues and challenges. In *Proceeding at the International IFSAM VIIIth World Congress*, p 28–30.

Sow, L. C., & Yang, H. (2015). Effects of salt and sugar addition on the physicochemical properties and nanostructure of fish gelatin. *Food Hydrocolloids*, *45*, 72–82.

Sow, L. C., Peh, Y. R., Perkerti, B. N., Fu, C., Bansal, N., & Yang, H. (2017). Nanostructure analysis and textural modification of tilapia fish gelatin affected by gellan and calcium chloride addition. *LWT - Food Science and Technology*, *85*, 137–145.

Verma, A., & Pandit, J. K. (2012). Comparative evaluation of Ca and Zn cross-linked gellan gum based floating beads. *Archives Des Sciences*, *65*, 75–84.

Vreeman, H. J., Snoeren, T. H. M., & Payens, T. A. J. (1980). Physicochemical investigation of κ-carrageenan in the random state. *Biopolymers*, *19*, 1357–1374.

Weng, W., Zheng, H., & Su, W. (2014). Characterization of edible films based on tilapia (*Tilapia zillii*) scale gelatin with different extraction pH. *Food Hydrocolloids*, *41*, 19–26.

Wu, B. C., & McClements, D. J. (2015). Microgels formed by electrostatic complexation of gelatin and OSA starch: Potential fat or starch mimetics. *Food Hydrocolloids*, *47*, 87–93.

Yang, H., & Wang, Y. (2009). Effects of concentration on nanostructural images and physical properties of gelatin from channel catfish skins. *Food Hydrocolloids*, *23*, 577–584.

Yang, H., Wang, Y., Jiang, M., Oh, J., Herring, J., & Zhou, P. (2007). 2-step optimization of the extraction and subsequent physical properties of channel catfish (*Ictalurus punctatus*) skin gelatin. *Journal of Food Science*, *72*, C188–C195.

Yang, H. (Ed.). (2014). *Atomic force microscopy (AFM): Principles, modes of operation and limitations*. N.Y., U.S.A.: Nova Science Publishers, Inc.

Yang, Z., Yang, H., & Yang, H. (2018). Effects of sucrose addition on the rheology and microstructure of κ-carrageenan gel. *Food Hydrocolloids*, *75*, 164–173.

Yu, G., Yan, X., Han, C., & Huang, F. (2013). Characterization of supramolecular gels. *Chemical Society Reviews*, *42*, 6697–6722.

Zhou, P., Mulvaney, S. J., & Regenstein, J. M. (2006). Properties of Alaska pollock skin gelatin: A comparison with tilapia and pork skin gelatins. *Journal of Food Science*, *71*, C313–C321.

Supporting Information

Additional Supporting Information may be found in the online version of this article at the publisher's website:

Fig. S1. Zeta potential changes of FG and PG at various pH.

*The isoelectric point of FG and PG were determined to be pH 7.79 and pH 7.92, respectively.

Fig. S2. FTIR spectra of PG, FG and the four selected formulations (FGG, FGG+, FGK, FGK+) *FGG (FG + 0.040% GE), FGG+ (FG + 0.025% GE + 3 mM $CaCl_2$), FGK (FG + 0.20 % KC) and FGK+ (FG + 0.18% KC + 5 mM KCl).